ADIPOSE TISSUE IN ATTENUATION AND SCATTERING CORRECTION IN MYOCARDIAL PERFUSION SPECT/CT: A PHANTOM STUDY

B. Guerreiro[1*], P. Pereira[1*], R. Rosa[1*], S. Valente[1,2], E. Sousa[3], P. Almeida[2,4],F. Branco[1,2], T. Freixo[2], F. D. Jonge[2], T. C. Ferreira[2], L. Vieira[3,4]

* Contributed equally to this research

(1) Escola Superior de Tecnologia e Saúde de Lisboa, Instituto politécnico de Lisboa, Lisboa, PORTUGAL

(2) Hospital Lusíadas, Departamento de Medicina Nuclear Lisboa, PORTUGAL

(3) GIReS- Escola Superior de Tecnologia e Saúde de Lisboa, Instituto politécnico de Lisboa, Lisboa, PORTUGAL

(4) Instituto de Biofísica e Engenharia Biomédica, Faculdade de Ciências, Universidade de Lisboa, Lisboa, PORTUGAL

2017/10/24

EANM'17 WORLD LEADING MEETING Vienna, Austria

NOTHING TO DECLARE

1. BACKGROUND

Myocardial Perfusion Imaging (MPI)

Risk stratification of coronary arterial disease (CAD) + therapeutic approach decision

Limitations

- **Attenuation Artifacts** → Corrected by computed tomography (CT)
- **Compton Scattering Artifacts** → Corrected by Dual or Triple energy window method (DEW and TEW)

Both influenced by adipose tissue (AT)

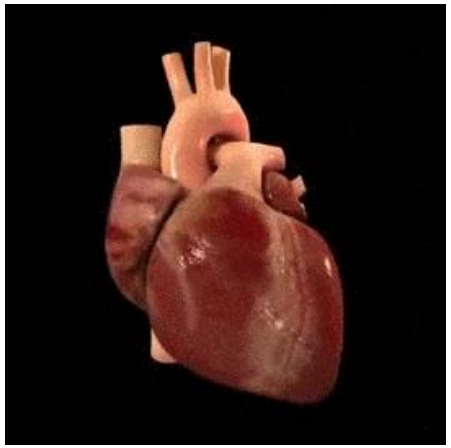

Assess the Influence of thoracic AT on cardiac SPECT/CT counts, after attenuation correction(AC) and scatter correction (SC)

Figueiredo SRR, Avaliação da viabilidade miocárdia pós-enfarte. 2013
Russell RR et al., Nuclear Cardiology: Present and Future. Curr Probl Cardiol, 2006
Stakhiv et al., Influence of Computed Tomography Attenuation Correction in Myocardial Perfusion Imaging : In Obese Population, 2015

2. METHODS

2.1. Materials and Methods

Used phantoms:

- Anthropomorphic thorax tissue equivalent

(RSD, Heart/ Thorax for Cardiac SPETC/PET, Alderson Phantom)

- Torso (approx. thickness = 35 millimetres, mm)

(RSD, Thorax Overlay phantom)

- Lung
- Liver
- Heart → 3 defects filled with ^{99m}Tc
  - a) superior: 3.36×10^{-2} MBq/mL in 41.70 mL
  - b) medial : 1.037×10^{-1} MBq/mL in 13.50 mL
  - c) inferior: 1.573×10^{-1} MBq/mL in 8.90 mL

→ 1.40 MBq per defect = 4.2 MBq in the heart

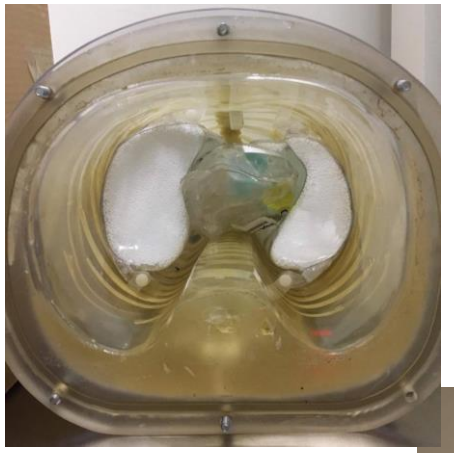

Fig. 1: Heart phantom placed between the lungs, inside the thorax phantom.

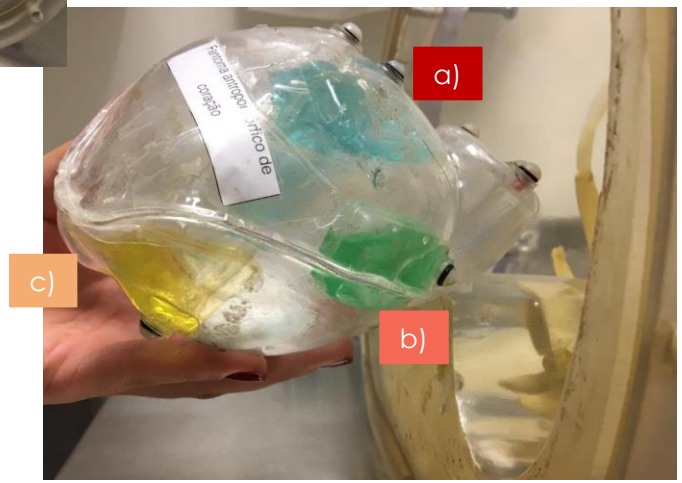

Fig. 2: Heart phantom with the superior (a), medial (b) and inferior (c) defects.

2. METHODS

2.1. Materials and Methods

Acquisitions:

1st) Thorax phantom

Fig. 3: Thorax phantom.

2nd) Thorax + Torso phantom

Fig. 4: Thorax and torso phantoms.

3rd) Thorax + Torso phantom + 1 AT layer (aprox. thickness = 10 mm)

Fig. 5: Thorax and torso phantom with one layer of AT.

4th) Thorax + Torso phantom + 3 AT layer (aprox. thickness = 30 mm)

Fig. 6: Thorax and torso phantom with three layers of AT.

2. METHODS

2.2. Image Acquisition Parameters

Gamma Camera:

Infinia Hawkeye 4, General Electrics Healthcare → 2 detectors and *Xeleris* workstation

Parameters

SPECT

- Collimators: Low energy high resolution (LEHR) in L mode
- Step and shoot mode: 180°, increase of 3°, right anterior oblique (RAO) → Left posterior oblique (LPO)
- Time per projection: 25 to 44 sec (*cf*. Table 1)
- ^{99m}Tc photopeak = 140 keV ; ±7.5% window
- Compton scatter photopeak = 120 keV; ±5% window
- Matrix: 64x64
- Zoom: 1.33

CT

- Slice thickness: 5 mm;
- 2.5 milliAmp;
- 2.0 rotations per minute;
- 140 kiloVolt;
- Standard filter;
- Matrix: 256x256;
- Pixel size:1.66 mm.

2. METHODS

2.2. Image Acquisition Parameters

Table 1: Time per scan in each acquisition.

Acquisition	Structures	Time (min)	
		SPECT	CT
1st	Thorax phantom 	12.50	5.00
2nd	Thorax phantom + torso phantom 	20.00	
3rd	Thorax phantom + torso phantom + 10 mm of adipose tissue 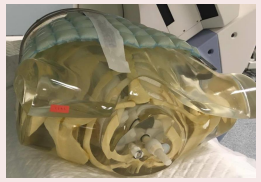	21.00	
4th	Thorax phantom + torso phantom + 30 mm of adipose tissue 	22.00	
		Total: 95.50	

2. METHODS

2.3. Image Reconstruction and Analysis

The scans were reconstructed using:

1) *Filtered Back Projection (FBP):*
   Butterworth Filter
   Slice Frequency = 0.48 cycles/pixel
   Order = 10

2) *Ordered Subset Expectation Maximization* (OSEM) + *Resolution Recovery* (RR)
   Slice Frequency = 0.48 cycles per pixel
   2.1.) OSEM RR;
   2.2.) OSEM RR AC;
   2.3.) OSEM RR AC SC.

Load to New:
3 frames with the most uptake per each defect

Circular regions of interest (ROI) per heart phantom regions (area = 10 pixel)

↓

Total counts, min, max, average and standard deviation (per ROI)

3. RESULTS AND DISCUSSION

Table 2: Average counts per pixel area and standard deviation, for the superior defect of the heart phantom, for all datasets with four types of reconstruction.

	Acquisition	1st 	2nd 	3rd 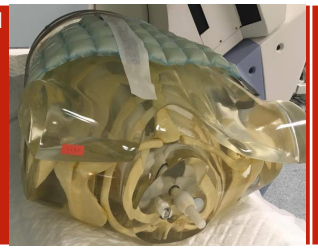	4th 
Superior Defect (average ± standard variation)	FBP	239.10 ± 61.38	156.80 ± 20.47	172.40 ± 24.03	142.30 ± 18.42
	OSEM RR	1743.30 ± 342.02	893.00 ± 209.60	1060.20 ± 274.80	919.60 ± 1984.00
	OSEM RR + AC	7803.70 ± 1518.14	5559.40 ± 1381.50	5851.2 ± 1664.90	7144.40 ± 1644.00
	OSEM RR + AC + SC	7325.50 ± 1456.10	5154.20 ± 1215.30	5426.80 ± 1477.50	6531.80 ± 1551.90

3. RESULTS AND DISCUSSION

Table 3: Average counts per pixel area and standard deviation, for the medial defect of the heart phantom, for all datasets with four types of reconstruction.

	Acquisition	1st 	2nd 	3rd 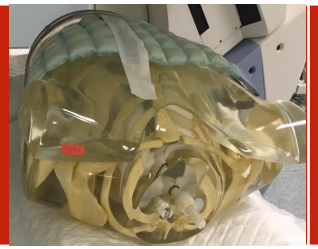	4th 
Medial Defect (average ± standard variation)	FBP	113.80 ± 28.26	99.00 ± 23.00	99.70 ± 16.89	65.20 ± 13.47
	OSEM RR	1008.80 ± 282.70	584.00 ±208.75	631.50 ± 189.90	526.60 ± 181.80
	OSEM RR + AC	4918.20 ± 2497.40	3991.40 ± 1380.40	3992.80 ± 1396.6	4740.00 ± 1411.90
	OSEM RR + AC + SC	4249.40 ± 1456.10	3511.40 ± 1336.10	3658.60 ± 1182.40	4068.90 ± 1411.30

3. RESULTS AND DISCUSSION

Table 4: Average counts per pixel area and standard deviation, for the inferior defect of the heart phantom, for all datasets with four types of reconstruction.

	Acquisition	1st 	2nd 	3rd 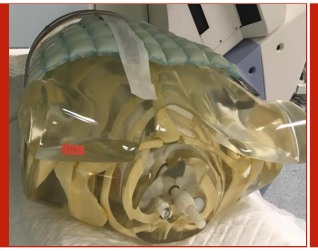	4th 
Inferior Defect (average ± standard variation)	FBP	338.00 ± 59.47	195.00 ± 47.57	170.40 ± 29.06	155.60 ± 42.12
	OSEM RR	2277.00 ± 755.30	1313.00 ± 383.90	1251.40 ± 330.60	1076.80 ± 430.40
	OSEM RR + AC	7569.10 ± 2514.70	5692.90 ± 1863.35	6140.40 ± 1590.00	6297.80 ± 1910.10
	OSEM RR + AC + SC	7280.90 ± 2461.20	5328.90 ± 1748.90	5646.10 ± 1531.20	5770.30 ± 1790.90

4. CONCLUSION

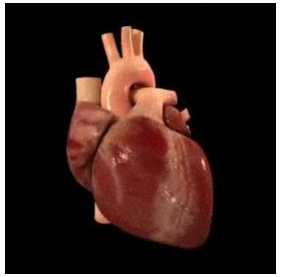

Evaluation of the influence of AT thickness on the counts rate after AC and SC

AC and SC effects are more notorious in bigger AT thicknesses.

↓

✓ The counts were almost totally recovered after AC and SC for the acquisition with the biggest AT thickness

✓ Is AC by CT and SC optimized for patients with less AT?

THANK YOU!

Acknowledge the financial support of Project IPL/2016/*CardiaCor*_ESTeSL

5. BIBLIOGRAPHIC REFERENCES

1. Figueiredo SRR. Avaliação da viabilidade miocárdia pós-enfarte. 2013;

2. Slart RHJ a, Bax JJ, van Veldhuisen DJ, van der Wall EE, Dierckx R a JO, Jager PL. Imaging Techniques in Nuclear Cardiology for the Assessment of Myocardial Viability. Int J Cardiovasc Imaging [Internet]. 2006 Feb 13;22(1):63–80.

3. Russell RR, Zaret BL. Nuclear Cardiology: Present and Future. Curr Probl Cardiol [Internet]. 2006 Sep;31(9):557–629.

4. Verberne HJ, Acampa W, Anagnostopoulos C, Ballinger J, Bengel F, De Bondt P, et al. EANM procedural guidelines for radionuclide myocardial perfusion imaging with SPECT and SPECT/CT: 2015 revision. Eur J Nucl Med Mol Imaging. 2015;42(12):1929–40.

5. Patton J a, Turkington TG. SPECT/CT physical principles and attenuation correction. J Nucl Med Technol. 2008;36(1):1–10.

6. Dvorak R a., Brown RKJ, Corbett JR. Interpretation of SPECT/CT Myocardial Perfusion Images: Common Artifacts and Quality Control Techniques. RadioGraphics. 2011 Nov;31(7):2041–57.

7. Kalender WA. Computed Tomography: Fundamentals, System Technology, Image Quality Applications. 3rd ed. Germany: Publicis Publishing; 2011.

8. Garcia E V., Esteves FP. Attenuation corrected myocardial perfusion SPECT provides powerful risk stratification in patients with coronary artery disease. J Nucl Cardiol [Internet]. 2009 Aug 3;16(4):490–2.

9. Raza H, Jadoon LK, Mushtaq S, Jabeen A, Maqbool M, Ain MU, et al. Comparison of non-attenuation corrected and attenuation corrected myocardial perfusion SPECT. Egypt J Radiol Nucl Med [Internet]. 2016 Sep;47(3):783–92.

10. Shawgi M, Tonge C, Lawson R. Attenuation correction of myocardial perfusion SPET in patients of normal body mass index. Hell J Nucl Med [Internet]. 2012;(November):215–9. Available from: http://europepmc.org/abstract/MED/23227459

11. Body Mass Index: Obesity and Overweight [Internet]. World Health Organization. 2016.

12. O. Stakhiv, I. Melo, M. Clarke, M. Aplin, N. Singh, K. Day, S. Dizdarevic, M. Jessop, P. Begley, E. Carolino, L. Vieira ES. INFLUENCE OF COMPUTED TOMOGRAPHY ATTENUATION CORRECTION IN MYOCARDIAL PERFUSION IMAGING, IN OBESE PATIENTS: CLASSIFICATION BY SEX AND BODY MASS INDEX. In: Maria Amélia Loja (IDMEC, ISEL/GIMOSM), Joaquim Infante Barbosa (IDMEC, ISEL/GIMOSM) JAR (ISEL/GIMOSM), editor. 3rd International Conference on Numerical and Symbolic Computation - Proceedings. Guimarães; 2017. p. 283–92.

13. Raza H, Jadoon LK, Mushtaq S, Jabeen A, Maqbool M, Ain MU, et al. Comparison of non-attenuation corrected and attenuation corrected myocardial perfusion SPECT. Egypt J Radiol Nucl Med. 2016 Sep;47(3):783–92.

14. Melo I, Begley P, Stakhiv O, Carolino E, Jessop M, Dizdarevic S, et al. Myocardial Perfusion Imaging in Obese Subjects : Influence of Adipose Tissue in Attenuation Correction with Computed Tomography. [Lisbon]: Lisbon School of Health Technology; 2015.

15. Pazhenkottil AP, Ghadri J-R, Nkoulou RN, Wolfrum M, Buechel RR, Küest SM, et al. Improved outcome prediction by SPECT myocardial perfusion imaging after CT attenuation correction. J Nucl Med. 2011 Feb;52(2):196–200.

16. Thompson RC, Heller G V., Johnson LL, Case JA, Cullom SJ, Garcia E V., et al. Value of attenuation correction on ECG-gated SPECT myocardial perfusion imaging related to body mass index. J Nucl Cardiol. 2005;12(2):195–202.

5. BIBLIOGRAPHIC REFERENCES

17. Ogawa K. Image distortion and correction in single photon emission CT. Ann Nucl Med. 2004;18(3):171–85.

18. Msaki P, Axelsson B, Dahl CM, Larsson SA. Generalized scatter correction method in SPECT using point scatter distribution functions. J Nucl Med. 1987 Dec;28(12):1861–9.

19. Laurette I, Zeng GL, Welch A, Beekman FJ, Kamphuis C, Frey EC, et al. Review and current status of SPECT scatter correction. Phys Med Biol Phys Med Biol. 2011;56(56):85–112.

20. Buvat I, De Sousa MC, Di Paola M, Ricard M, Lumbroso J, Aubert B. Impact of scatter correction in planar scintimammography: a phantom study. J Nucl Med. 1998 Sep;39(9):1590–6.

21. Xiao J, de Wit TC, Staelens SG, Beekman FJ. Evaluation of 3D Monte Carlo-based scatter correction for 99mTc cardiac perfusion SPECT. J Nucl Med. 2006 Oct;47(10):1662–9.

22. Narayanan MV, Pretorius PH, Dahlberg ST, Leppo JA, Botkin N, Krasnow J, et al. Evaluation of scatter compensation strategies and their impact on human detection performance tc-99m myocardial perfusion imaging. IEEE Trans Nucl Sci. 2003 Oct;50(5):1522–7.

23. El Fakhri G, Buvat I, Benali H, Todd-Pokropek A, Di Paola R. Relative impact of scatter, collimator response, attenuation, and finite spatial resolution corrections in cardiac SPECT. J Nucl Med. 2000 Aug;41(8):1400–8.

24. Radiology Support Devices | Heart/Thorax for Cardiac SPECT/PET.

25. Platts EA, North TL, Pickett RD, Kelly JD. Mechanism of uptake of technetium-tetrofosmin. I: Uptake into isolated adult rat ventricular myocytes and subcellular localization. J Nucl Cardiol [Internet]. [cited 2017 Jun 12];2(4):317–26.

26. Darcourt J, Booij J, Tatsch K, Varrone A, Walker Z, Laere K Van. EANM procedure guidelines for brain neurotransmission SPECT using 123 I-labelled dopamine transporter ligands , version 2. 2009.

27. Oliveira ML, Seren MEG, Rocha FC, Brunetto SQ, Ramos CD, Button VLSN. Attenuation correction effects on SPECT/CT procedures: Phantoms studies. Proc Annu Int Conf IEEE Eng Med Biol Soc EMBS. 2013;2324–7.

28. Links JM, DePuey EG, Taillefer R, Becker LC. Attenuation correction and gating synergistically improve the diagnostic accuracy of myocardial perfusion SPECT. J Nucl Cardiol. 9(2):183–7.

29. R H. Attenuation correction eternal dilemma or real improvement. J Nucl Med Mol Imaging. 2005;49(1):30–42.

30. Tamam M, Mulazimoglu M, Edis N, Ozpacaci T. The Value of Attenuation Correction in Hybrid Cardiac SPECT/CT on Inferior Wall According to Body Mass Index. World J Nucl Med [Internet]. 2016 [cited 2017 Jun 13];15(1):18–23.

31. Saffar MH, Oloomi S, Knoll P, Taleshi H. A new approach to scatter correction in SPECT images based on Klein _ Nishina equation. 2013;21(1):19–25.

32. Blokland KJ a K, de Vos tot Nederveen Cappel WH, van Eck-Smit BLF, Pauwels EKJ. Scatter correction on its own increases image contrast in Tl-201 myocardium perfusion scintigraphy, but does it also improve diagnostic accuracy? Ann Nucl Med. 2003;17(8):725–31.

33. Pourmoghaddas A, Vanderwerf K, Ruddy TD, Glenn Wells R. Scatter correction improves concordance in SPECT MPI with a dedicated cardiac SPECT solid-state camera. J Nucl Cardiol. 2015 Apr;22(2):334–43.